Band Electronic Structure Study of Compound $(ET)_2ICl_2$ in Two Structural Modifications

Dae Bok Kang

Department of Chemistry, Kyungsung University, Pusan 608-736
Received September 19, 1993

The crystals of β- and β′-$(ET)_2ICl_2$ have a modified structure of organic superconductor β-$(ET)_2I_3$. These salts possess strictly different physical properties : the β phase is a metal but the β′ phase is a semiconductor. Our band electronic structure calculations show that the β phase is somewhat anisotropic 2D metal and the β′ phase with the 1D character in electronic structure is magnetic insulating, in good agreement with experimental indications.

Introduction

A large number of salts of the donor radical cation BEDT-TTF (bis(ethylenedithio)tetrathiafulvalene **1**, also known as ET) have been found with electrical conductivities ranging from insulators to superconductors.[1] These salts typically contain the layered networks of ET molecules consisting of ET molecular stacks, separated by layers of anions. A very important aspect of their structures is that the ET compounds contain two-dimensional (2D) networks of short *S*···*S* interactions which increase their dimensionality and intermolecular electronic communication. However, it should be noted here that the 2D molecular network does not always lead to 2D electronic structure because the magnitude of the intermolecular interaction between the ET molecules depends on not only short intermolecular *S*···*S* contact distance but also the contribution from both σ- and π-type highest occupied molecular orbital (HOMO) interactions between ET molecules based on geometric considerations.

The crystals of β- and β′-$(ET)_2ICl_2$ were obtained electrochemically.[2,3] On two of the polymorphic modifications of composition $(ET)_2ICl_2$, Shibaeva *et al.* have found substantially different electrical properties : one of them (the β phase) is metallic to very low temperatures but are not superconducting, and the other (the β′ phase) is a semiconductor at all temperatures from room temperature on down. The β phase salt is a quasi-2D metal but differs in structure from the β phase superconductors in that the layer of adjacent stacks of ET donor molecules is nearly coplanar. We find that the Fermi surface of this salt shows an unusual coexistence of both 1D and 2D surfaces. This suggests that electrical transport in this salt is more complicated than it is in the simpler 1D or 2D organic salt. Unlike β phase salt with both 1D and 2D Fermi surfaces, β′ phase has a 1D-like electronic structure with the valence band spanning a narrow energy range (*i.e.*, ~0.3 eV). This difference comes from the anisotropy of the interaction between the ET molecules within a donor layer of β′ phase which is weak but larger along only one direction. In this connection, Williams *et al.*[4] have reported that the β′ phase is a 1D metal on the basis of ESR observation. But the conductivity measurement work by Shibaeva *et al.* shows that this salt is a semiconductor.[2] This discrepancy will be discussed in view of the effect of Coulomb interaction of electrons leading to their localization on the dimerized ET molecules in this paper.

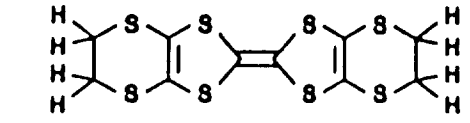

BEDT-TTF (ET)

1

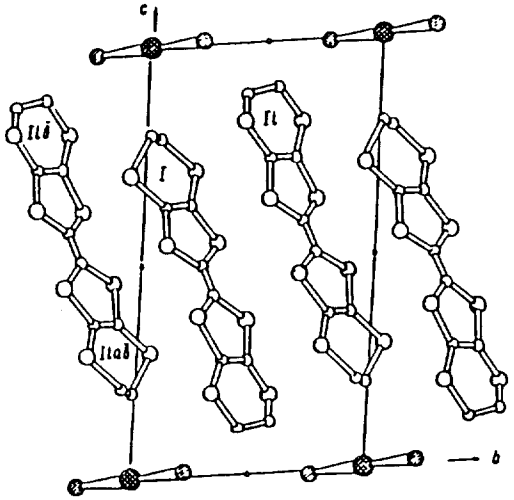

Figure 1. Projection view of the β-$(ET)_2ICl_2$ structure along the *a*-axis direction (Reference 2).

In order to better understand the electronic structures of these two phases and hence their electrical properties, we carried out tight-binding band electronic structure calculations[5] for their ET networks determined by Shibaeva *et al.*[2,3]

Crystal Structure and Physical Property Description

The crystal structures of β- and β′-$(ET)_2ICl_2$ are shown in Figures 1 and 2, respectively, and the basic crystallographic data for the crystals are presented in Table 1. With almost identical density of the crystals, in β′ phase the parameter *c* is substantially lower compared with the β phase, while the periods *a* and *b* are significantly higher. These parameters are undoubtedly important for crystal packing, and indirectly contribute to the relative measure of the ex-

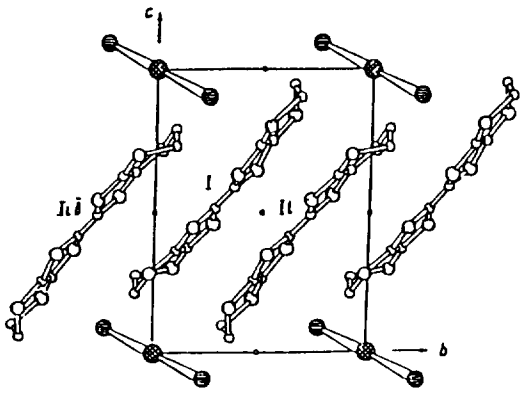

Figure 2. Projection view of the β′-$(ET)_2ICl_2$ structure along the *a*-axis direction (Reference 2).

Table 1. Crystallographic Data for the β and β′ phases of $(ET)_2ICl_2$[a]

Parameter	Phase	
	β′	β
a, Å	6.638	5.734
b	9.760	8.979
c	12.906	16.66
α, deg	87.11	82.18
β	100.93	76.59
γ	98.62	76.43
V, Å^3	811.5	808.2
Space group	$P\bar{1}$	$P\bar{1}$
Z	1	1
$d_{calc.}$ g/cm^3	1.99	2.00

[a] Taken from References 2 and 3.

tent of interactions between ET molecules. The packing motifs of the 2D ET networks for these two phases are compared in Figures 3 and 4. A common feature of both networks is that stacks of ET molecules interact with one another in the crystallographic *ab* plane, and a given ET molecule of one stack is positioned parellel to and between the planes of two ET molecules in an adjacent stack. However, there is a great difference in this stacking motif between those two phases. In β′-$(ET)_2ICl_2$, as shown in Figure 3, the donor stack consists of ET dimers with a relative displacement of ET molecules along the long in-plane molecular axis within a dimer which do not form a smooth ET molecule layer but protrude into the anion sheets to such an extent that the anions are greatly separated from each other. The ET dimers do not overlap each other. There are no shortened intermolecular *S*···*S* contacts less than the sum of the van der Waals radii (3.6 Å) within the donor stacks. The manner in which adjacent ET molecules overlap in the donor stack of the β phase in Figure 4 is characterized by large displacements along their short in-plane molecular axes. All intermolecular *S*···*S* contacts within the stack are greater than the analogous contacts between stacks and not less than the van der Waals distance. On the other hand, numerous short inter-

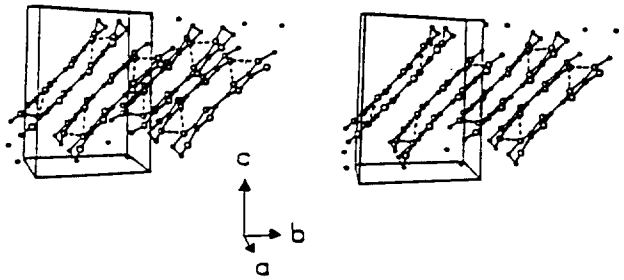

Figure 3. Stereoview of the crystal packing of donor molecular layers in β′-$(ET)_2ICl_2$. Thermal ellipsoids are shown at an arbitrary scale. Dashed lines denote intermolecular *S*···*S* contacts less than 3.6 Å. For simplicity, the hydrogen atoms are not shown.

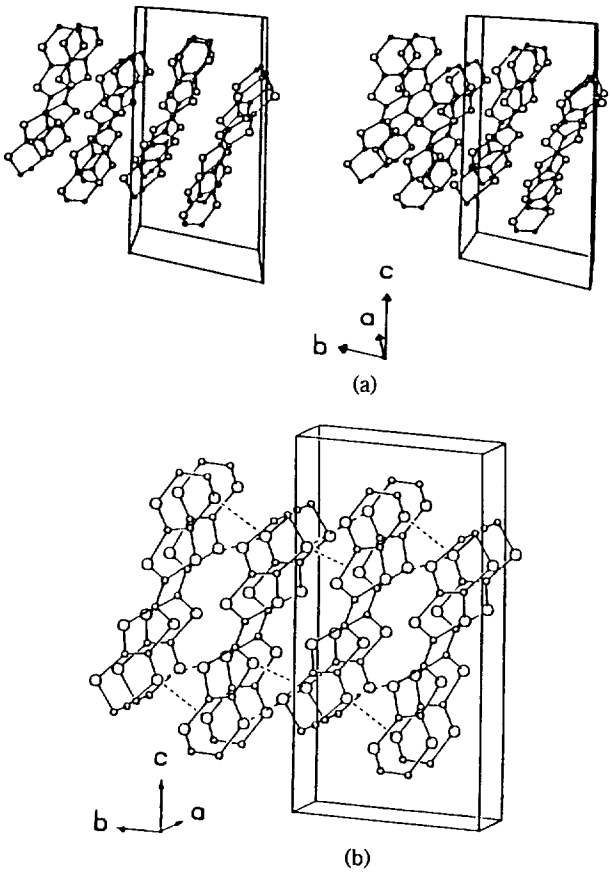

Figure 4. Stereoscopic (a) and perspective (b) view of the crystal packing of donor molecular layers in β-$(ET)_2ICl_2$. Dashed lines denote intermolecular *S*···*S* contacts less than 3.6 Å. For simplicity, the hydrogen atoms are not shown.

stack *S*···*S* contacts are found both in the β and in the β′ phase. In the β′ phase, each ET molecule has eight contacts (3.439-3.539 Å) with two molecules of the adjacent stacks. In the β phase, each ET molecule has ten contacts (3.335-3.660 Å) with four molecules of the adjacent stacks. Eight of these ten contacts come from the two ET molecules lying in the plane close to a given ET molecular plane. In crystals of the β′ phase the positional disorder of one of the terminal ethylene groups of the ET molecule is found, while in the β phase both groups are ordered. We note that in β phase

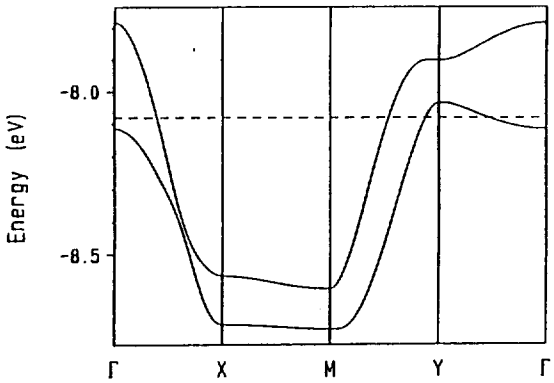

Figure 5. Dispersion relations for the highest two occupied bands of β-$(ET)_2ICl_2$, where the dashed line refers to the Fermi level. Γ, X, Y, and M represent the wave-vector points (0, 0), ($a^*/2$, 0), (0, $b^*/2$), and ($a^*/2$, $b^*/2$) of the first Brillouin zone, respectively.

the parameter a is significantly shortened and thus $S\cdots S$ contacts between stacks are highly shortened. The nature of overlapping of adjacent molecules whithin the ET stack of β-$(ET)_2ICl_2$ differs from that of β-$(ET)_2I_3$. In the β-$(ET)_2I_3$ structure there are more short interstack $S\cdots S$ contacts between ET molecules which are not located in the same plane. In contrast, most short corresponding contacts in β-$(ET)_2ICl_2$ occur for two ET molecules lying in the plane close to the ET molecular plane. This means that in β-$(ET)_2ICl_2$ the packing motif of the ET molecules in the donor layer is less isotropic than in β-$(ET)_2I_3$.

The physical properties of the β and β′ phases of $(ET)_2ICl_2$ differ substantially.[2] The β phase has high conductivity of the metallic type ($\sigma_{300\,K}=200$ ohm$^{-1}\cdot$cm^{-1}) along a. The temperature dependence of the resistance is metallic in nature but the transition to the superconducting state is not observed down to 1.3 K. The stability of the metallic state at very low temperatures might be connected with the quasi-two-dimensional character of its electronic structure.[6] We note that the conductivity of β-$(ET)_2ICl_2$ crystals measured at room temperature originates from the highly shortened $S\cdots S$ contacts between stacks. The conductivity measurement of β′-$(ET)_2ICl_2$ shows that it is a semiconductor.[2] The conductivity at room temperature is low ($\sigma_{300\,K}=10^{-2}$ ohm$^{-1}\cdot$cm^{-1}) and is found to decrease exponentially with a reduction in temperature with activation energy of 0.1 eV. The presence of semiconductor properties in the β′ phase can be explained in terms of the donor molecule networks composed of weakly interacting chains of strongly dimerized ET molecules along the b-axis direction while the interactions in other directions are significantly weak. This structural feature leads to a 1D-like weak band dispersion responsible for electron localization on the dimerized ET molecules due to the effect of Coulomb repulsion between electrons. Similar situation has been observed earlier in the 1D compound β-$(BPDT\text{-}TTF)_2I_3$.[7]

Band Electronic Structure

To examine the origin of the electrical properties of β- and β′-$(ET)_2ICl_2$, extended Hückel tight-binding band calculations[5] were performed on the basis of the crystal structures of these salts reported in references 2 and 3. We employ all valence atomic orbitals of double-zeta Slater type orbitals for carbon and sulfur atoms in the calculations.[5] A double-zeta orbital is given by a linear combination of a diffuse and a contracted orbital. A single-zeta orbital is generally closer in orbital extension to the contracted than to the diffuse component of the corresponding double-zeta orbital. The diffuse component leads to larger intermolecular overlap than does the contracted component, so that double-zeta orbitals provide larger intermolecular overlap than do single-zeta orbitals.

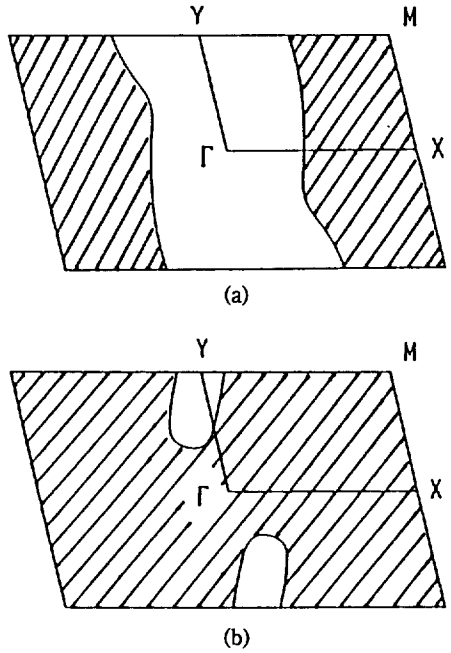

Figure 6. The fermi surfaces associated with the upper band and the lower band of Figure 5 in (a) and (b), respectively. The wavevectors in the shaded and unshaded regions of the first Brillouin zone lead to the occupied and unoccupied levels of these bands, respectively, and the boundary between the two wavevector regions is the Fermi surface.

Figure 5 shows the dispersion relations of the highest two occupied bands for the structure of β-$(ET)_2ICl_2$ which are mainly constructed from the HOMO's of two ET molecules in each unit cell. With the formal oxidation $(ET)_2^+$, there are three electrons per unit cell that remain to fill the two bands so that the upper band is half-filled. The valence band is more dispersive along the Γ→X or M→Y direction than along the Γ→Y direction. The upper band shows a strong 1D character since its bottom portion is occupied for those wavevectors in the vicinity along X→M, so that this band leads to the open Fermi surface shown in Figure 6a. The top portion of the lower band is empty for those wavevectors around Y. Thus the lower band leads to a hole pocket of the closed Fermi surface (in the extended zone scheme) shown in Figure 6b. This Fermi surface is elongated along the direction approximately perpendicular to the a^* direction. Therefore, the electrical conductivity of β-$(ET)_2ICl_2$ is expected to be higher along the a* direction, *i.e.*, the ET interstack

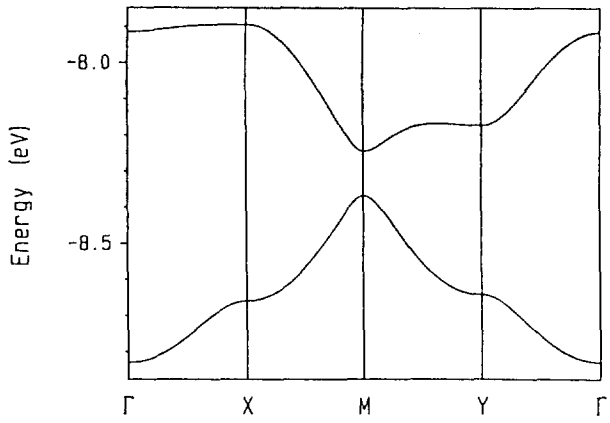

Figure 7. Dispersion relations for the highest two occupied bands of β′-$(ET)_2ICl_2$. Γ, *X*, *Y*, and M represent the wave-vector points (0, 0), ($a^*/2$, 0), (0, $b^*/2$), and ($a^*/2$, $b^*/2$) of the first Brillouin zone, respectively.

direction. This anisotropic behavior is related to the fact that the donor layer of β-$(ET)_2ICl_2$ consists of a number of highly shortened *S*···*S* contacts between ET stacks and the intermolecular *S*···*S* contacts with the less effective overlap mode within the stack.

Shown in Figure 7 are the highest two occupied bands calculated for the ET molecule layer of β′-$(ET)_2ICl_2$. The two bands are primarily derived from the HOMO of each ET molecule and are different in character from those calculated for β-$(ET)_2ICl_2$. The upper band is half-filled because of the formal oxidation $(ET)_2^+$ per unit cell, and it is dispersive along the Γ→Y or X→M direction but nearly flat along the Γ→X direction. The weak dispersion of this band results from the fact that interactions between two separate dimeric units in a given stack are extremely weak compared to weak interstack interactions, while interactions within the dimeric unit are much stronger because of effective σ-type overlap. The half-filled band is assumed to be metallic if each occupied level has two electrons. This kind of band-filling is energetically favorable in terms of occupying low-lying orbitals. When the Coulomb repulsion between electrons dominates over orbital energy contribution, however, a Mott insulating state of the half-filled band becomes more stable than its metallic state despite of the presence of partially filled bands in a one-electron band picture.[8] In general, a system with the partially filled band is expected to be a Mott insulator when its bandwidth is small compared with the on-site Coulomb repulsion.[8] The insulating property of a Mott insulator originates from electron localization caused by electron-electron repulsion. Therefore, it is not surprising to speculate that the donor interactions of β′-$(ET)_2ICl_2$ can provide a narrow enough band susceptible to Mott electron localization. The experimental findings[2] that the β′ phase exhibits semiconductor properties support the viewpoint that it may be energetically more favorable for electrons to remain localized on each ET dimer unit due to the narrow width of the band. The spin arrangement of localized electrons may have a long-range order as in the ferromagnetic or in the antiferromagnetic state. However, the recent ESR study on β′-$(ET)_2ICl_2$ has suggested that this salt is a 1D metal and undergoes a metal-insulator (MI) transition below 22 K.[4] These findings are not consistent with the proposal[2] that this salt is a Mott insulator with spin density. Furthermore, axial rotation photographs of the X-ray diffraction intensities about *a*, *b*, and *c* axes in β′-$(ET)_2ICl_2$ at 15 K (*i.e.*, below its T_{MI}=22 K) are found to reveal no evidence of superlattice.[4] Consequently, it is more probable that the quasi-1D β′-$(ET)_2ICl_2$ is magnetic insulating in nature, as in the case of β-(BPDT-TTF)$_2I_3$.

Concluding Remarks

We have examined the relationships between the structures and properties of the two polymorphic modifications of $(ET)_2ICl_2$. The strict differences in the properties of those two arise from the relative arrangements of nearest-neighbor ET molecules in their planar ET networks and consequently the different dimensionality of the electronic systems. According to the present band electronic structure calculations, the β phase contains both 1D and 2D Fermi surfaces. The 2D Fermi surface associated with the lower band of Figure 5 is somewhat anisotropic in two dimensions since it is elongated along the direction approximately perpendicular to the Γ→X direction, while the 1D Fermi surface associated with the upper band of Figure 5 is open along the intrastack direction Γ→Y. Thus the stability of the metallic state with respect to the MI transition observed for the β phase is probably connected with the quasi-2D character of the lower band. As shown in Figure 7, the anisotropy of the dispersion relations of the valence band with narrow width in β′ phase suggests the 1D character in electronic structure. The semiconducting property of this salt at room temperature and below is explained by electron localization in the stacks of $(ET)_2^+$ dimer cations.

Acknowledgment. This paper was supported by NON DIRECTED RESEARCH FUND, Korea Research Foundation, 1991.

Appendix. The atomic parameters used in the calculations are as follows: S, 3*s*: $H_{ii}=-20.0$ eV, $\zeta_1=2.662$, $c_1=0.5564$, $\zeta_2=1.688$, $c_2=0.4874$; 3*p*: $H_{ii}=-13.3$ eV, $\zeta_1=2.338$, $c_1=0.5212$, $\zeta_2=1.333$, $c_2=0.5443$. C, 2*s*: $H_{ii}=-21.4$ eV, $\zeta_1=1.831$, $c_1=0.7616$, $\zeta_2=1.153$, $c_2=0.2630$; 2*p*: $H_{ii}=-11.4$ eV, $\zeta_1=2.730$, $c_1=0.2595$, $\zeta_2=1.257$, $c_2=0.8025$. H, 1*s*; $H_{ii}=-13.6$ eV, $\zeta=1.30$. A set of 66 k points was chosen for the Fermi surface calculations of half the first Brillouin zone.

References

1. For a review, see: Williams, J. M.; Wang, H. H.; Emge, T. J.; Geiser, U.; Beno, M. A.; Leung, P. C. W.; Carlson, K. D.; Thorn, R. J.; Schultz, A. J.; Whangbo, M.-H. *Prog. Inorg. Chem.* **1987**, *35*, 51.
2. Buravov, L. I.; Zvarykina, A. V.; Ignat'ev, A. A.; Kotov, A. I.; Laukhin, V. N.; Makova, M. K.; Merzhanov, V. A.; Rozenberg, L. P.; Shibaeva, R. P.; Yagubskii, E. B. *Izv. Akad. Nauk SSSR, Ser. Khim.* **1988**, 2027.
3. Shibaeva, R. P.; Rozenberg, L. P.; Yagubskii, E. B.; Ignat' ev, A. A.; Kotov, A. I. *Dolk. Akad. Nauk SSSR* **1987**, *292*, 1405.
4. Emge, T. J.; Wang, H. H.; Leung, P. C. W.; Rust, P. R.; Cook, J. D.; Jackson, P. L.; Carlson, K. D.; Williams, J. M.; Whangbo, M.-H.; Venturini, E. L.; Schirber, J. E.; Azevedo, L. J.; Ferraro, J. R. *J. Am. Chem. Soc.* **1986**, *108*,

695.
5. Hoffmann, R. *J. Chem. Phys.* **1963**, *39*, 1397. We used double-zeta Slater type orbitals adapted from: Clementi, E.; Roetti, C. *At. Data Nucl. Data Tables* **1974**, *14*, 177. The H_{ij} values were calculated from a modified Wolfsberg-Helmholtz formula; Ammeter, J. H.; Bürgi, H.-B.; Thibeault, J. C.; Hoffmann, R. *J. Am. Chem. Soc.* **1978**, *100*, 3686. See Reference 9 for details.
6. Whangbo, M.-H. In *Electron Transfer in Biology and the Solid State: Inorganic Compounds with Unusual Properties*; King, R. B., Ed.; American Chemical Society: Washington, DC, 1990; p 269.
7. Kobayashi, H.; Takahashi, M.; Kato, R.; Kobayashi, A.; Sasaki, Y. *Chem. Lett.* **1984**, 1331.
8. (a) Mott, N. F. *Metal-Insulator Transitions*; Barnes and Noble: New York, 1977; (b) Brandow, B. H. *Adv. Phys.* **1977**, *26*, 651; (c) Whangbo, M.-H. *Acc. Chem. Res.* **1983**, *16*, 95; *J. Chem. Phys.* **1979**, *70*, 4963; (d) Whangbo, M.-H. In *Crystal Chemistry and Properties of Low-Dimensional Solids*; Rouxel, J., Ed.; Reidel: Dordrecht, The Netherlands, 1986; p 27.
9. Whangbo, M.-H; Williams, J. M.; Leung, P. C. W.; Beno, M. A.; Emge, T. J.; Wang, H. H.; Carlson, K. D.; Crabtree, G. W. *J. Am. Chem. Soc.* **1985**, *107*, 5815.

Synthesis and Structure of 1,2,3,4,5-Pentamethylcyclopentadienyl-1,4-Diphenyltetraazabutadiene Complexes of Rhodium and Iridium

Cheolki Paek, Jaejung Ko*, Sangook Kang†, and Patrick J. Carrol‡

Department of Chemical Education, Korea National University of Education, Chungbuk 363-791
†Department of Chemistry, College of National Science, Korea University, Chochiwon 339-700
‡Department of Chemistry, University of Pennsylvania, Philadelphia, Pennsylvania 19104-6323
Received November 24, 1993

Monomeric rhodium and iridium-diaryltetrazene complexes Cp*M(RNN=NNR)(Cp*=1,2,3,4,5-pentamethylcyclopentadienyl; M=Rh, Ir; R=Ph, 4-tolyl) have been synthesized from $[Cp^*MCl_2]_2$(M=Rh, Ir) and **2** equiv. of $[Li(THF)_x]_2(RN_4R)$ in benzene. We have determined the crystal structure of (η^5-pentamethylcyclopentadienyl)diphenyltetrazene iridium by using graphite-monochromated Mo-$K_\alpha$radiation. The compound was crystallized in the monoclinic space group $P2_1/c$ with $a=13.781(3)$, $b=9.035(1)$, $c=17.699(3)$ Å, and $\beta=111.93(1)°$. An X-ray crystal structure of complex **1** showed a short N(2)-N(3) distance (1.265 Å) consistent with the valence tautomer A with Ir(III) rather than Ir(I). All complexes are highly colored and decompose on irradiation at 254 nm. Electrochemical studies show that complex **1** displays a quasi-reversible reduction.

Introduction

Since the discovery of $[Fe(R_2N_4)(CO)_3]$ in 1967[1], transition-metal tetraazadiene complexes have been reported, including derivatives of Ni, Co, Ir, Rh, and Pt by coupling reactions between an organic azide and a metal complex in a low oxidation state or tetrazenido dianion and transition-metal dihalide complex.[2-9]

Transition-metal tetraazadiene complexes have attacted interest because of their novel bonding mode and the possibility of dinitrogen extrusion. It has been suggested that resonance structures *A* and *B* contribute to the overall structure of tetrazene complexes.[10,11] The formal valence structure *A* or *B* in the complex was adopted by the extent the delocalization of π-electron density in the metallacycles and the role of the metal *d* orbitals in bonding. Backbonding from the metal to the lowest ligand π-acceptor orbital would induce the bond length variation found in structure *A*. In particular, the structure *A* gives us a good model of nitrogen extrusion because of the weak bond strength of N(1)-N(2). The fact stimulates us to explore the preparation of the complexes of the type *A* by changing the ligand attached to the transition-metal. Herein we reported the syntheses of transition-metal tetraazadiene complexes by the reaction of Rh and Ir complexes with tetrazenido dianion.

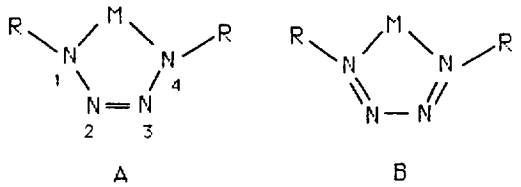

Experimental Section

All manipulations of air-sensitive materials were carried out under an argon atmosphere with use of standard Schlenk or vacuum line technique or a Mebraun MB150 glovebox. ^{1}H-NMR spectra were recorded on a Bruker WM-250 spectrometer in $CDCl_3$. Chemical shifts are given in parts per million relative to TMS for ^{1}H-NMR spectra. IR spectra were obtained by using a Perkin-Elmer 1310 instrument. Mass spectra were measured on a high resolution VG70-VSEG